Eur. Phys. J. B **57**, 1–7 (2007)
DOI: 10.1140/epjb/e2007-00149-8

THE EUROPEAN PHYSICAL JOURNAL B

Magnetotransport of lanthanum doped $RuSr_2GdCu_2O_8$ – the role of gadolinium

M. Požek[1,a], A. Dulčić[1], A. Hamzić[1], M. Basletić[1], E. Tafra[1], G.V.M. Williams[2,3], and S. Krämer[2,b]

[1] Department of Physics, Faculty of Science, University of Zagreb, P.O. Box 331, 10002 Zagreb, Croatia
[2] 2. Physikalisches Institut, Universität Stuttgart, 70550 Stuttgart, Germany
[3] Industrial Research, P.O. Box 31310, Lower Hutt, New Zealand

Received 20 December 2006 / Received in final form 27 April 2007
Published online 25 May 2007 –

Abstract. Strongly underdoped $RuSr_{1.9}La_{0.1}GdCu_2O_8$ has been comprehensively studied by dc magnetization, microwave measurements, magnetoresistivity and Hall resistivity in fields up to 9 T and temperatures down to 1.75 K. Electron doping by La reduces the hole concentration in the CuO_2 planes and completely suppresses superconductivity. Microwave absorption, dc resistivity and ordinary Hall effect data indicate that the carrier concentration is reduced and a semiconductor-like temperature dependence is observed. Two magnetic ordering transitions are observed. The ruthenium sublattice orders antiferromagnetically at 155 K in low applied magnetic fields, and the gadolinium sublattice orders antiferromagnetically at 2.8 K. The magnetoresistivity in this compound exhibits a complicated temperature dependence due to the occurence of the two magnetic orders and spin fluctuations. It is shown that the ruthenium magnetism influences the conductivity in the RuO_2 layers while the gadolinium magnetism influences the conductivity in the CuO_2 layers. The magnetoresistivity is isotropic above 4 K, but it becomes anisotropic close to the gadolinium antiferromagnetic order temperature.

PACS. 74.72.-h Cuprate superconductors – 74.25.Fy Transport properties – 74.25.Ha Magnetic properties – 74.25.Nf Response to electromagnetic fields

1 Introduction

The observation of magnetic order with a ferromagnetic (FM) component and superconductivity (SC) in the ruthenate cuprates is an intriguing issue that has motivated a number of studies especially since it has been reported that superconductivity and the magnetic order may coexist [1]. It has been argued that the coexistence of the competing order parameters occurs via a spontaneous vortex phase [1,2] in a similar way as in the Ru1222 compounds [3].

In $RuSr_2RCu_2O_8$ (R = Eu,Gd) the low field magnetic ordering at $T_M \approx 133$ K is predominantly antiferromagnetic (AFM) with spin-canting leading to a small ferromagnetic component [4–7]. With increasing magnetic field, the ferromagnetic component increases [4,5,7] presumably due to spin-flop transitions [5]. Also, it has recently been reported that a small fraction of ferromagnetic nanoparticles may appear dispersed in the antiferromagnetic lattice of $RuSr_2RCu_2O_8$ [8].

There is a general agreement that superconductivity is associated with the CuO_2 layers and magnetic order with the RuO_2 layers when R = Eu. It has been shown that both kinds of layers contain delocalized carriers [9], with the coupling between the CuO_2 and RuO_2 layers being weak [10,11]. Furthermore, nuclear magnetic resonance measurements [12] have shown that there is a weak exchange coupling between Ru and Cu, while electron paramagnetic resonance measurements have shown that there is also a weak exchange coupling between Ru and Gd [13].

There is still an open debate concerning the nature of the low field antiferromagnetic order in the ruthenium sublattice. Neutron scattering experiments suggest G-type antiferromagnetism where the Ru spins are aligned along the c-axis [4,6], whereas zero-field nuclear magnetic resonance measurements suggest that the spins are aligned in the ab-plane [9]. In addition to the low-field AFM ordering of the ruthenium sublattice, the gadollinium sublattice orders in G-type antiferromagnetism at 2.8 K [4]. The dipolar fields from the AFM ordered ruthenium sublattice do not exactly cancel at the gadollinium site because of the spin canting [6].

The coupling between the magnetic orders in the Ru- and Gd-sublattices was indicated from magnetization measurements [5,6], but the effect of this coupling on

[a] e-mail: mpozek@phy.hr
[b] *Present address:* Grenoble High Magnetic Field Laboratory, CNRS, B.P. 166, 38042 Grenoble Cedex 9, France.

the transport properties has not been studied because the pure compound is superconducting at the temperatures of interest.

In order to study the evolution of the magnetic order from high to low temperatures, and its impact on the transport properties, one needs to eliminate the superconducting state. For this purpose, we have prepared a La-doped sample, $RuSr_{1.9}La_{0.1}GdCu_2O_8$ (5% of La on the strontium site). The lattice parameters in the substituted compound are changed only by a very small amount with respect to the parent compound, but the electronic structure is greatly affected. The replacement of Sr^{2+} by La^{3+} reduces the hole concentration in CuO_2 planes below that required for the occurence of superconductivity (less than 0.05 holes per Cu) [14].

2 Experimental details

The $RuSr_{1.9}La_{0.1}GdCu_2O_8$ ceramic sample was prepared by the procedure described previously [15].

Resistivity, magnetoresistivity and Hall effect measurements were carried out using the standard six-contact configuration using the rotational sample holder and the conventional ac technique (22 Hz, 1 mA), in magnetic fields up to 9 T. The magnetoresistivity was measured with magnetic field (**H**) and current (**I**) in both, transversal (**H** $\perp$ **I**) and longitudinal (**H** $\parallel$ **I**) configurations. The temperature was controlled with carbon-glass and platinum thermometers in temperature swept resistivity measurements, while a capacitance thermometer was used in magnetic field sweeps at constant temperatures.

The characterization of the samples by both, dc and ac magnetization measurements was done using a SQUID magnetometer.

Microwave measurements were carried out in an elliptical ${}_e\mathrm{TE}_{111}$ copper cavity operating at 9.3 GHz. The sample was mounted on a sapphire sample holder and positioned in the cavity center where the microwave electric field has a maximum. The temperature of the sample could be varied from liquid helium to room temperature. Measurements were made with dc magnetic fields of up to 8 T. The details of the detection scheme are given elsewhere [16]. The measured quantities were $1/2Q$, the total losses of the cavity loaded by the sample, and $\Delta f/f$, the relative frequency shift with respect to the starting point in the measurement. They are simply related to the surface impedance of the material Z_s, which depends on the complex conductivity $\widetilde{\sigma}$ and complex relative permeability $\widetilde{\mu}_r$. The total microwave impedance comprises both nonresonant resistance and resonant spin contributions.

3 Results and analyses

Figure 1a shows dc magnetization of $RuSr_{1.9}La_{0.1}GdCu_2O_8$. It is similar to the magnetization measured previously in the pure compound [10]), but with a slightly higher magnetic ordering transition temperature $T_{Ru} \approx$ 155 K in RuO_2 planes, and no sign of superconductivity in CuO_2 planes down to 1.8 K. The upturn in magnetization below 25 K follows the Curie-Weiss law $C/(T-\Theta)$ with Θ between 2 and 5 K. It is due to the enhanced paramagnetism of Gd ions. Antiferromagnetic ordering of the Gd sublattice appears at $T_{Gd} = 2.8$ K (inset).

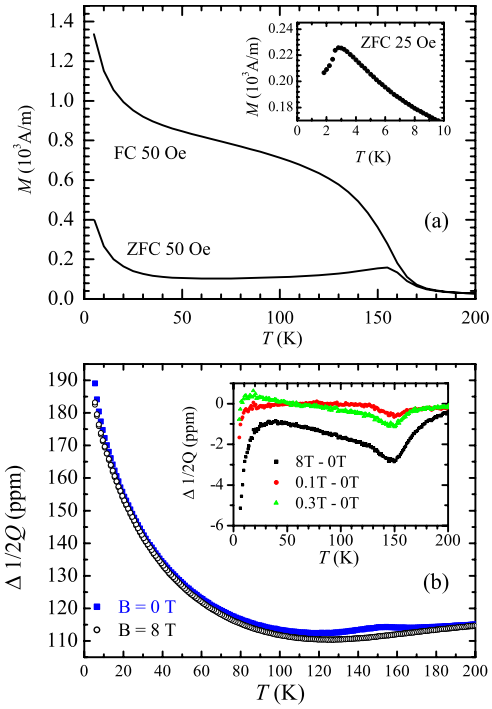

Fig. 1. (a) Field cooled (FC) and zero field cooled (ZFC) magnetization of the ceramic sample measured in dc magnetic field of 50 Oe. Inset: ZFC magnetization at low temperatures, measured in dc field of 25 Oe; (b) microwave absorption of the ceramic sample measured in zero field (full squares) and in $B =$ 8 T (open circles). The observed peak at 155 K disappears at fields higher than 1 T. The inset shows the differences between the microwave absorption measured at several field values and the absorption at zero field (microwave magnetoresistance).

The temperature dependence of the microwave absorption in zero field and in $B = 8$ T is shown in Figure 1b. The high temperature microwave absorption is about two times larger than that of the pure compound, indicating that the conductivity is lower in the La-doped compound. The zero field microwave absorption shows a peak at $T_{Ru} \approx 155$ K which disappears at fields higher than 1 T. The inset shows microwave magnetoresistance for three different fields. This behaviour is qualitatively and quantitatively equivalent to that observed in the pure compound [10]. At lower temperatures the absorption rises, in contrast to the absorption in the superconducting parent compound. This rise is a combined effect due to the sample resistivity and paramagnetic resonance from the Gd ions. The magnetic field dependence of the microwave complex frequency shift at 5.5 K is shown in Figure 2. The signal is dominated by electron paramagnetic resonance (EPR) from the Gd^{3+} ions. Namely, when a conducting sample is placed at the position of the maximum microwave

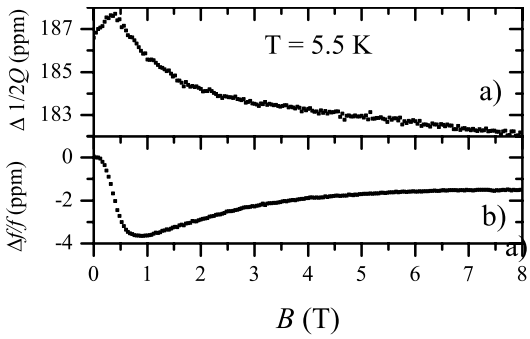

Fig. 2. Magnetic field dependence of the complex frequency shift at $T = 5.5$ K: (a) imaginary part of the complex frequency shift (absorption); (b) real part of the complex frequency shift (dispersion). The signals are dominated by electron spin resonance from the Gd^{3+} ions.

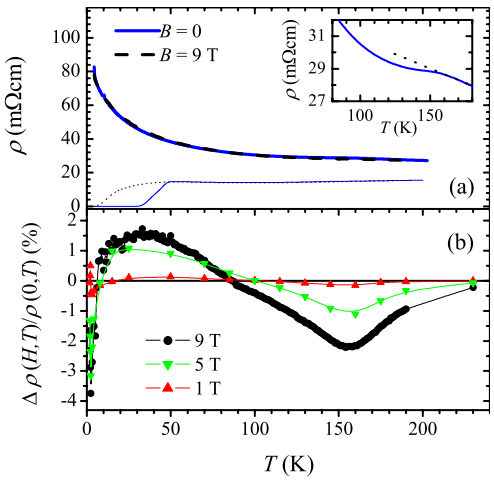

Fig. 3. (a) Resistivity of $RuSr_{1.9}La_{0.1}GdCu_2O_8$ in zero field and at $B = 9$ T. The resistivity of the parent compound $RuSr_2GdCu_2O_8$ [10] is also plotted by thinner lines for comparison. The inset shows the zero field resistance curve in an enlarged scale. The dotted line is the extrapolation of the temperature dependence of the resistivity from higher to lower temperatures. (b) Transversal magnetoresistivity at three different fields. The lines are guides to the eye.

electric field, the induced surface currents create a nonvanishing **B** inside the sample [17]. The observed EPR line is wide and the signal becomes detectable below 45 K. This gadollinium EPR signal was obscured by the effects of superconducting weak links in the bulk pure compound, but it was observable in the powdered sample of the same pure compound [10].

The resistivity in zero field and in $B = 9$ T is shown in Figure 3a. At high temperatures the resistivity is roughly two times larger than in the pure compound (also shown in Fig. 3a). The contribution of intergranular regions to the resistivity cannot be excluded, especially at lower temperatures. However, we note that the Hall measurements, shown later in this paper, clearly show that the number of carriers in the substituted compound is reduced with respect to that found in the pure compound. The kink that can be seen in the zero field resistivity curve at 155 K corresponds to the peak observed in the microwave absorption, and in zero field cooled (ZFC) magnetization curves. It is the sign of the antiferromagnetic ordering in the RuO_2 planes. The relative transversal magnetoresistivity $\Delta\rho(H,T)/\rho(0,T)$ at applied magnetic fields of 1 T, 5 T, and 9 T ($\Delta\rho(H,T) = \rho(H,T) - \rho(0,T)$) is shown in Figure 3b. It can be seen that the magnetoresistivity at 9 T shows a pronounced minimum at 155 K, becomes positive at 85 K, shows a maximum at 30 K, and becomes negative again below 10 K. Note that similar behaviour is also present in the microwave absorption (inset to Fig. 1b). We aim to study in detail this complex temperature behaviour.

Figure 4 shows transversal magnetoresistivity versus magnetic field in a large temperature range from 230 K down to 1.75 K. The curves are grouped in subsets according to the physical processes that dominate in each of the temperature ranges.

The behaviour at high temperatures from 230 K down to 160 K is shown in Figure 4a. In this temperature range, there can occur ferromagnetic spin fluctuations without any long range magnetic order. The application of an external field leads to a net thermal average moment and

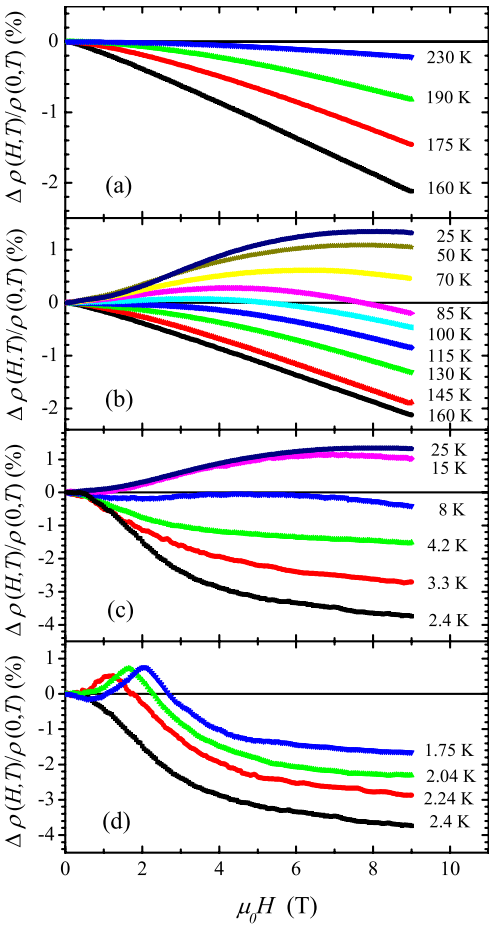

Fig. 4. Relative transversal magnetoresistivity: (a) above 160 K; (b) between 25 K and 160 K; (c) between 2.4 K and 25 K; (d) below 2.4 K.

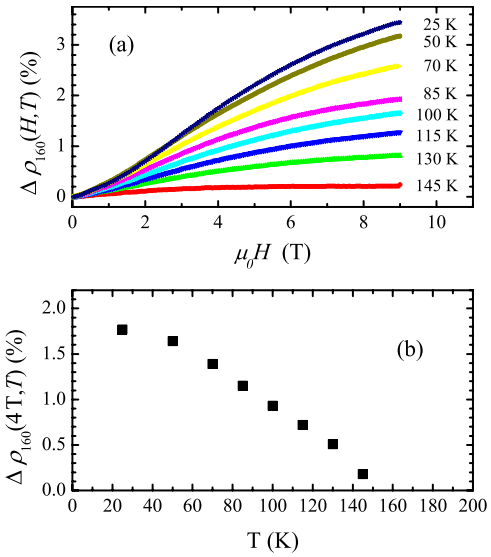

Fig. 5. (a) Net magnetoresistivity at temperatures between 25 K and 145 K (the curve at 160 K is subtracted). We denote $\Delta\rho_{160}(H,T) = \Delta\rho(H,T)/(\rho(0,T)) - \Delta\rho(H,160\text{ K})/(\rho(0,160\text{ K}))$; (b) the net magnetoresistivity at 4 T for temperatures below 160 K.

a concomittant reduction in the carrier scattering, thus yielding negative magnetoresistivity.

Antiferromagnetic long range order appears only below 155 K in zero field, or in very small applied fields, as can be seen in the magnetization curves in Figure 1a. With the onset of antiferromagnetic order, the magnetoresistivity curves in Figure 4b become progressively less negative. This behaviour is opposite to that in Figure 4a, and indicates that a different physical process sets in. In order to interprete the MR curves below the magnetic ordering temperature, it is useful to look first at the behaviour of the zero field resistivity (inset to Fig. 3a). When the AFM order sets in, the resistivity drops below the values that might have been expected from the extrapolation of the temperature dependence observed above the transition (dotted line in the inset of Fig. 3a). Similar behaviour is also seen in the zero field microwave absorption in Figure 1b. Since no appreciable change of the measured Hall coefficient is observed in the vicinity of 155 K (see later in this paper), we believe that the presently described observations can be interpreted as a clear evidence that the carrier scattering is reduced due to the onset of the AFM order. Having this in mind, we can now turn our attention again to the magnetoresistivity curves in Figure 4b. The increasing field first reduces the AFM order parameter, thus yielding an increase in the carrier scattering. Therefore, the magnetoresistivity curve at 145 K shows a relative increase with respect to the 160 K curve. When the long range AFM order is destroyed, the spin system is in the paramagnetic phase, and the increasing applied field favours ferromagnetic fluctuations. This explains why the magnetoresistivity remains negative. However, as the temperature is lowered further on, the AFM order parameter becomes larger. Below 100 K, it is strong enough that the initial rise of the magnetoresistivity curves dominates in Figure 4b. It appears that much larger applied fields would be required in order to destroy the AFM order parameter.

It is also known that an increased magnetic field can lead to spin canting, which yields an FM component. This growing FM component tends to decrease the carrier scattering, so that the magnetoresistivity curves acquire a negative slope at high enough fields. It is difficult to distinguish between this long range FM component and the field induced FM fluctuations that remain after any long range order parameter is destroyed. However, we observe in Figure 4b that the negative slopes which appear at high fields in low temperature curves are not bigger in absolute values than the slope of the curve at 160 K. Hence, it seems that the long range FM component, due to canting of the AFM order, does not exceed the field induced FM fluctuations.

We believe that it is possible to separate AFM and FM contributions to the magnetoresistivity, at least in an approximate way. We have subtracted MR curve at 160 K from MR curves at lower temperatures, and the result is shown in Figure 5a. If one assumes that the FM contribution to the magnetoresistivity does not change appreciably below 160 K, the plotted curves represent an AFM contribution to the magnetoresistivity due to the ruthenium sublattice. The AFM order parameter in the ruthenium sublattice is gradually reduced with increasing magnetic field, and the introduced disorder makes a positive contribution to the magnetoresistivity. At lower temperatures, the zero field AFM order parameter becomes larger, so that the corresponding curves in Figure 5a also show a larger rise. At high enough fields, when the AFM order is completely destroyed, the curves in Figure 5a saturate.

The evolution of the ruthenium AFM order parameter can be followed in Figure 5b, where the AFM contribution to the MR at 4 T is plotted. This order parameter practically saturates at lower temperatures, and it is reasonable to assume that the ruthenium contribution to the MR curves does not change appreciably at temperatures below 25 K. The same conclusion would be reached if the points were plotted at some other field value.

The magnetoresistivity curves at still lower temperatures show yet another interesting feature below 25 K (cf. Fig. 4c). A negative contribution appears in the magnetoresistivity curves at 15 K (slightly) and 8 K (more pronounced), and superimposes on the total signal. It becomes dominant as the temperature is lowered down to 2.8 K. Given the saturation trend observed in Figure 5, it is unlikely that a dramatic change occurs in the ordering of the ruthenium subsystem below 25 K. On the other hand, gadolinium spins exhibit enhanced paramagnetism below 25 K, as seen from the magnetization curves in Figure 1a, and the microwave absorption in the inset to Figure 1b. The paramagnetism from the Gd ions is so strong at 5.5 K that electron spin resonance can be observed (Fig. 2) even without the common field modulation technique. Hence, we ascribe the observed negative contribution to the magnetoresistivity in Figure 4c to a precursor of the AFM ordering of the Gd spin

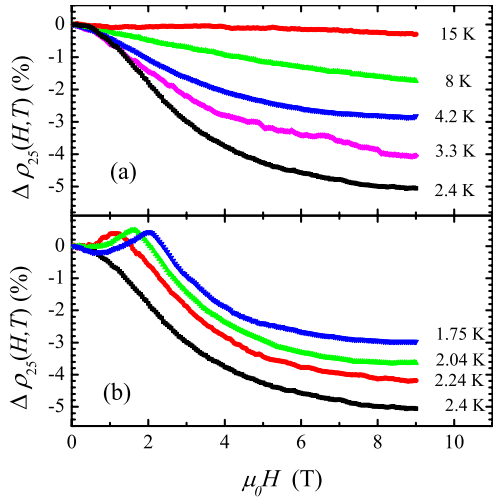

Fig. 6. Differences between transversal magnetoresistivity ($\Delta\rho_{25}(H,T) = \Delta\rho(H,T)/\rho(0,T) - \frac{\Delta\rho(H,25\ \mathrm{K})}{\rho(0,25\ \mathrm{K})}$) at various temperatures (The curve at 25 K is subtracted): (a) net magnetoresistivity at temperatures between 2.4 K and 15 K; (b) net magnetoresistivity at temperatures between 1.75 K and 2.4 K.

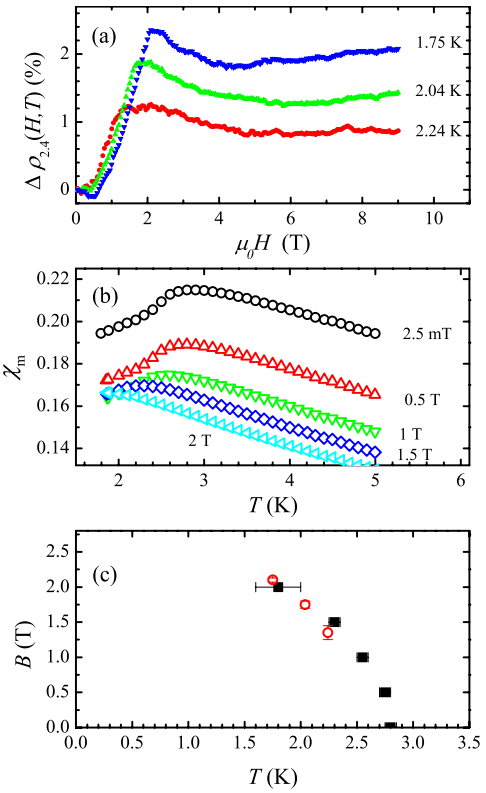

Fig. 7. (a) Net magnetoresistivity at temperatures below 2.4 K when magnetoresistivity at 2.4 K is subtracted ($\Delta\rho_{2.4}(H,T) = \Delta\rho(H,T)/\rho(0,T) - \Delta\rho(H,2.4\ \mathrm{K})/\rho(0,2.4\ \mathrm{K})$); (b) low-temperature magnetic susceptibility for several applied magnetic fields; (c) peak positions of the magnetic susceptibility in b, full squares) and saturation fields of the AFM magnetoresistivity in a, open circles).

subsystem. To distinguish the evolution of the gadolinium spin subsystem contribution from the already saturated ruthenium contribution, we can subtract the MR curve at 25 K from MR curves at lower temperatures. The results are shown in Figure 6. The evolution above 2.4 K (Fig. 6a) is qualitatively similar to the behaviour of the Ru subsystem above 160 K observed in Figure 4a. The gadolinium spin subsystem exhibits strong paramagnetism as a precursor to AFM ordering. The application of an external magnetic field stimulates parallel alignment of the Gd spins, thus reducing spin disorder and carrier scattering. The largest negative magnetoresistivity in Figure 6 is observed at 2.4 K, slightly below the AFM ordering temperature of the Gd spin subsystem.

The effect of the increasing AFM order parameter at still lower temperatures is seen in Figure 6b. Qualitatively, this behaviour is similar to that of the ruthenium subsystem below 155 K. The initial rise of the magnetoresistivity is due to the destruction of the long range AFM order of the Gd subsystem. At higher fields, the negative component of the magnetoresistivity prevails. In analogy with the ruthenium subsystem, we assume that the negative magnetoresistivity is due to the field induced FM fluctuations, and assume that this component does not change appreciably below 2.4 K. Hence, we subtract the curve at 2.4 K from the MR curves at lower temperatures, and the result is shown in Figure 7a. The initial rise of the magnetoresistivity appears to be analogous to the behaviour already seen in Figure 5a for the ruthenium governed magnetoresistivity.

In order to check the correspondence of the magnetoresistivity to the phase diagram of the Gd spin sublattice, we have performed a series of magnetization measurements at low temperatures. The magnetic susceptibility at various applied fields is shown in Figure 7b. The AFM transition temperature is suppressed by the magnetic field, and completely disappears in fields higher than 2 T. The peak positions are plotted in the phase diagram shown in Figure 7c. The field values where the AFM contribution to the magnetoresistivity reaches a maximum in Figure 7a, are also plotted in Figure 7c as open symbols. It is obvious that the two observed features are well correlated. Therefore we can identify the maxima in Figure 7a with the field induced transition from antiferromagnetic to the paramagnetic phase of the Gd spin subsystem.

In order to extract additional information from the magnetoresistivity, we have measured it in both, longitudinal ($\mathbf{H} \parallel \mathbf{I}$) and transversal ($\mathbf{H} \perp \mathbf{I}$) configurations, so that the anisotropy can be determined. The detected anisotropy in the magnetoresistivity is very small for temperatures above 4 K, similar to the observation in pure compound [10]. However, below 4 K a significant anisotropy appears between the transversal and longitudinal magnetoresistivity. The two curves taken at $T = 2.04$ K are shown in Figure 8a. The anisotropy at other temperatures below 4 K is qualitatively similar to that in Figure 8a. Their common feature is that the anisotropy does not show up at low magnetic fields where the magnetoresistivity is positive. This is the region where the AFM order of the Gd spins prevails. At higher fields a gradual

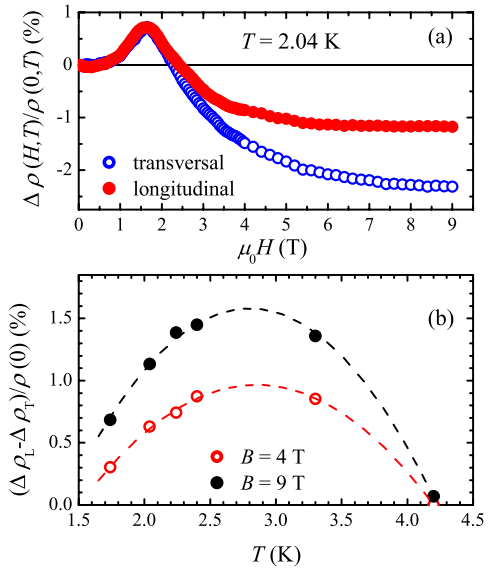

Fig. 8. (a) Transversal and longitudinal magnetoresistivity at $T = 2.04$ K; (b) temperature dependence of anisotropy at $B = 4$ T (opened circles) and $B = 9$ T (full circles). The plotted parabolas serve as guides to the eyes.

difference between the longitudinal and transversal magnetoresistance develops. It is well-known that anisotropy in magnetoresistance is a common feature of ferromagnets [18], and we suggest that the present observation is yet another evidence that ferromagnetic fluctuations related to the Gd spin subsystem develop at higher fields. The evolution of the anisotropy with temperature is also interesting. Figure 8b shows data taken at 4 T and 9 T. The anisotropy reaches its maximum around $T_{Gd} = 2.8$ K. Obviously, it corresponds to the gadolinium magnetic ordering temperature.

The Hall resistivity has also been measured, and data for some high temperatures are shown in Figure 9. The Hall resistivity is linear up to 9 T for all measured temperatures, and the deduced Hall constant is very weakly temperature dependent. Its value was roughly two times larger than the high field Hall constant of the undoped sample, indicating a reduced number of carriers. The Hall resistivity of the undoped sample at 124.5 K is shown by the dashed line in Figure 9. We note that in the present study there is no significant nonlinearity of the Hall resistance, i.e. there is no clear evidence of an extraordinary Hall effect. In our previous paper, the observation of the extraordinary Hall effect was taken as an important evidence that the RuO_2 layers are conducting in the pure sample [10]. The lack of the extraordinary Hall effect in the La-doped sample need not, however, be taken as a proof that the RuO_2 layers are not conducting. It is rather likely that the absence of nonlinearity in the Hall resistivity in Figure 9 is due to a smaller, and more linear magnetization in this sample. Thus, based only on the Hall resistivity, we can neither prove nor reject the conduction in the RuO_2 layers. However, we believe that the MR data strongly suport the conductance in both, the RuO_2 and CuO_2 layers.

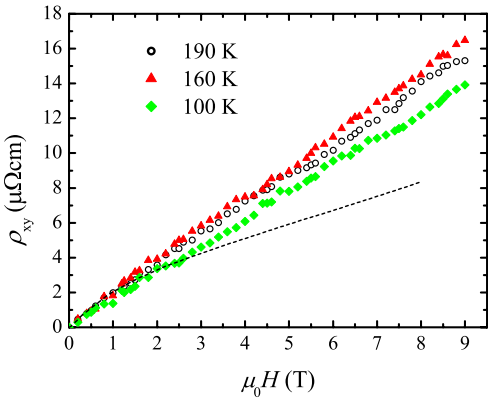

Fig. 9. Hall resistivity at three different temperatures. The Hall resistivity of the undoped sample at 124.5 K is shown by the dashed line [10].

4 Discussion

The extensive measurements carried out in this work on the La-doped Ru-1212:Gd sample have yielded complex results. We shall attempt to interprete the various features in the experimental data as being related to the crystal structure of $RuSr_2GdCu_2O_8$.

The ruthenium magnetic ions are relatively far away from the conducting CuO_2 planes. As pointed out by Picket et al.[19], the ruthenium magnetization lies within the t_{2g} orbitals that do not directly couple to the Cu $d_{x^2-y^2}$ or Cu s orbitals. Hence, their influence on the conduction in the CuO_2 layers is small, but they certainly influence the conduction in their own RuO_2 planes.

Almost all of the magnetoresistivity above 25 K, seen in Figures 4a and 4b is due to processes in the RuO_2 planes, which are both, conducting and magnetic.

On the other hand, gadolinium magnetic ions are close to the conducting CuO_2 planes. Strongly localized gadolinium f states do not significantly influence the relaxation rates of conduction electrons in the distant RuO_2 layers but may have some effect in the nearby conducting copper planes. Therefore, we ascribe the evolution of the magnetoresistivity below 25 K, seen in Figure 6, to the scattering processes in the CuO_2 planes.

It is worth noting that the magnetoresistivity at all temperatures is a weak effect, which amounts at most to a few percent. The present results show that the ordering of the ruthenium sublattice at higher temperatures does not significantly affect the scattering rate of the carriers, simply because the scattering is already strong. As for the gadolinium spin ordering at low temperatures, it has a small effect on magnetoresistivity because gadolinium is not embeded in the conducting plane.

The side position of Gd^{3+} ions with respect to the conducting CuO_2 plane can also explain the observed anisotropy of magnetoresistivity. The magnetoresistivity anisotropy usually occurs when the ions with nonspherical distribution of charge are embeded into a conducting system. A charge carrier encounters an object with a different cross section depending on whether it arrives with

its **k**-vector parallel or perpendicular to the moment of the non-spherical ion [18]. The scattering potential includes an isotropic attractive potential term V_0, a spin dependent exchange interaction term V_{ex}, and a quadrupolar Coulomb term V_{qd} [20]. Since the Gd^{3+} ion has a spherical f-shell, the quadrupolar contribution to the anisotropy should be excluded. The only possible origin of the MR anisotropy could then be due to the already mentioned position of the Gd^{3+} ions. The conducting electrons feel different scattering potential V_{ex} when Gd spins are oriented parallel to the conducting planes or perpendicular to them.

5 Conclusions

In conclusion, the replacement of 5% Sr^{2+} ions by La^{3+} ions in $RuSr_2GdCu_2O_8$ further decreases doping in the CuO_2 planes in the already underdoped parent compound to a level where superconductivity is completely suppressed. The number of carriers is strongly reduced as revealed by the Hall resistance. DC and microwave resistivities are two times larger than in the pure compound at higher temperatures and show semiconductor-like behaviour at lower temperatures.

However, there still remain two conducting layers that are effectively decoupled. The conducting RuO_2 layers are influenced by magnetic ordering of the Ru spins as already observed in the parent compound. We detect and explain the influence of gadolinium magnetism on the conductivity. Gadolinium localized spins do not alter the electronic band structure of the CuO_2 layers, but may influence the relaxation rates of normal-state electrons when superconductivity is destroyed by other means (underdoping).

We acknowledge funding support from the Croatian Ministry of Science, Education and Sports (projects No. 119-1191458-1022 "Microwave Investigations of New Materials" and no. 119-1191458-1023 "Systems with spatial and dimensional constraints: correlations and spin effects"), the New Zealand Marsden Fund, the New Zealand Foundation for Research Science and Technology, and the Alexander von Humboldt Foundation. M.P. thanks to Dr. Ivan Kupčić for valuable discussions.

References

1. C. Bernhard, J.L. Tallon, E. Brücher, R.K. Kremer, Phys. Rev. B **61**, 14960 (2000)
2. C. Bernhard, J.L. Tallon, Ch. Neidermayer, Th. Blasius, A. Golnik, E. Brücher, R.K. Kremer, D.R. Noakes, C.E. Stronach, E.J. Ansaldo, Phys. Rev. B **59**, 14099 (1999)
3. E.B. Sonin, I. Felner, Phys. Rev. B **57**, 14000 (1998)
4. J.W. Lynn, B. Keimer, C. Ulrich, C. Bernhard, J.L. Tallon, Phys. Rev. B **61**, 14964 (2000)
5. G.V.M. Williams, S. Krämer, Phys. Rev. B **62**, 4132 (2000)
6. J.D. Jorgensen, O. Chmaissem, H. Shaked, S. Short, P.W. Klamut, B. Dabrowski, J.L. Tallon, Phys. Rev. B **63**, 054440 (2001)
7. H. Takagiwa, J. Akimitsu, H. Kawano-Furukawa, H. Yoshizawa, J. Phys. Soc. Jpn **70**, 333 (2001)
8. M.R. Cimberle, R. Masini, F. Canepa, G. Costa, A. Vecchione, M. Polichetti, R. Ciancio, Phys. Rev. B **73**, 214424 (2006)
9. Y. Tokunaga, H. Kotegawa, K. Ishida, Y. Kitaoka, H. Takagiwa, J. Akimitsu, Phys. Rev. Lett. **86**, 5767 (2001)
10. M. Požek, A. Dulčić, D. Paar, A. Hamzić, M. Basletić, E. Tafra, G.V.M. Williams, S. Krämer, Phys. Rev. B **65**, 174514 (2002)
11. J.E. McCrone, J.L. Tallon, J.R. Cooper, A.C. McLaughlin, J.P. Attfield, C. Bernhard, Phys. Rev. B **68**, 064514 (2003)
12. S. Krämer, G.V.M. Williams, Physica C **377**, 282 (2002)
13. A. Fainstein, E. Winkler, A. Butera, J.L. Tallon, Phys. Rev. B **60**, 12597 (1999)
14. P. Mandal, A. Hassen, J. Hemberger, A. Krimmel, A. Loidl, Phys. Rev. **B65**, 144506 (2002)
15. G.V.M. Williams, H.K. Lee, S. Krämer, Phys. Rev. B **67**, 104514 (2003)
16. B. Nebendahl, D.-N. Peligrad, M. Požek, A. Dulčić, M. Mehring, Rev. Sci. Instrum. **72**, 1876 (2001)
17. D.-N. Peligrad, B. Nebendahl, C. Kessler, M. Mehring, A. Dulčić, M. Požek, D. Paar, Phys. Rev. B **58**, 11652. (1998)
18. I.A. Campbell, A. Fert, in *Ferromagnetic Materials*, edited by E.P. Wohlfarth (North-Holland, 1982), Vol. 3, p. 747
19. W.E. Picket, R. Weht, A.B. Shick, Phys. Rev. Lett. **83**, 3713 (1999)
20. A. Fert, R. Asomoza, D.H. Sanchez, D. Spanjaard, A. Friedrich, I.A. Campbell, Phys. Rev. B **16**, 5040 (1977)